

Force Spectroscopy Study of Langmuir–Blodgett Asymmetric Bilayers of Phosphatidylethanolamine and Phosphatidylglycerol

Laura Picas,[†] Carme Suárez-Germà,[†] M. Teresa Montero,[‡] and Jordi Hernández-Borrell^{*,†,‡}

Departament de Físicoquímica, Facultat de Farmàcia, Universitat de Barcelona, 08028-Barcelona, Spain, and Institut de Nanociència i Nanotecnologia de la Universitat de Barcelona (IN²UB), 08028-Barcelona, Spain

Received: November 16, 2009; Revised Manuscript Received: January 28, 2010

Phosphatidylethanolamine (PE) and phosphatidylglycerol (PG) are the main components of the inner membrane of *Escherichia coli*. Mixtures of PE and PG mimicking the proportions found in *E. coli* have been extensively used to reconstitute transmembrane proteins as lactose permease (LacY) in proteoliposomes because in this environment the protein shows maximal activity. Hence, the study of the physicochemical properties of this phospholipid matrix becomes of potential interest. In previous studies,^{1,2} we used atomic force microscopy (AFM) and force spectroscopy (FS) to study the topographic and nanomechanical properties of supported lipid bilayers (SLBs) of 1-palmitoyl-2-oleoyl-*sn*-glycero-3-phosphoethanolamine (POPE) and of POPE and 1-palmitoyl-2-oleoyl-*sn*-glycero-3-phosphoglycerol (POPG) (3:1, mol/mol). The study reported here was extended for completeness to asymmetric SLBs obtained by the Langmuir–Blodgett (LB) method. Thus, we prepared SLBs with the proximal leaflet extracted at 30 mN·m⁻¹ and the distal leaflet extracted at 25 mN·m⁻¹. We prepared SLBs with both leaflets with same composition (POPG/POPG), and also with the proximal leaflet of POPE and the distal leaflet of POPG or POPE:POPG (3:1, mol/mol). The topography of the SLBs acquired in liquid was compared with the topography of the monolayers acquired in air. Breakthrough (F_y) and adhesion forces (F_{adh}) of SLBs were extracted from force curves. The values obtained are discussed in terms of the possible involvement of the nanomechanical properties of the SLBs in membrane protein insertion. The results provide means for the observation that insertion of LacY in POPE:POPG (3:1, mol/mol) occurs preferentially in the fluid phase, which is the phase with the lower F_y and the higher F_{adh} .

Introduction

The mechanism of energy transduction in biological membranes is still not understood. As postulated by Peter Mitchell,^{3,4} accumulation of a large number of solutes against a concentration gradient is driven by the proton electrochemical gradient ($\Delta\tilde{\mu}_{H^+}$). In the bioenergetic field, the transport protein, lactose permease (LacY) of *Escherichia coli*, is considered the paradigm of the secondary transport proteins that couple the energy stored in the $\Delta\tilde{\mu}_{H^+}$ into a concentration gradient.⁵ Little is known about the molecular origin of the proton that triggers transduction.

The physiological activity of transmembrane proteins, however, may depend on the physicochemical properties of neighboring phospholipids. Such dependence has been demonstrated in the case of, among others, β -hydroxybutyrate dehydrogenase, Ca²⁺-ATPase⁶ and melibiose permease.⁷ Apart from its function, LacY requires phosphatidylethanolamine (PE) for its correct folding and for maintaining its correct topology (ref 8 and references therein). In this regard, PE is relevant to other proteins such as LmrP⁹ or channels such as KcsA,¹⁰ which suggests a general role of PE in membrane transport processes. Moreover, all integral membrane proteins are surrounded by a layer of phospholipids, the annular region, which provides the adequate lateral pressure and fluidity to seal the membrane during the changes in the protein during transport events.⁵ Recently, by using Förster resonance energy transfer (FRET) techniques, we determined that the annular region of LacY is

slightly enriched in PE, but that phosphatidylglycerol (PG), the other main component of the *E. coli* membrane, is also present.¹¹ Actually, under very different conditions, the headgroup composition of the phospholipids present in the inner membrane of *E. coli* is relatively constant (70–80% PE, 20–25% PG, and 5–7% of CL).^{12,13} Remarkably, the main phospholipids present, PE and PG, both participate in hydrogen bonding and are possible candidates for interaction with the protein, hypothetically providing protons. In a similar hypothesis to that posed for diphosphatidylglycerol (Cardiolipin),¹⁴ PE and PG at the annular region might be involved in the maintenance of $\Delta\tilde{\mu}_{H^+}$.

Furthermore, bacterial cell membranes have laterally heterogeneous distribution of lipid molecules.¹⁵ This is the case of PE and PG, for which the use of pyrene-labeled phospholipids¹⁶ and atomic force microscopy (AFM)² has clearly demonstrated that they form laterally segregated domains. Specifically, the lateral segregation for the hetero-acid phospholipids, 1-palmitoyl-2-oleoyl-*sn*-glycero-3-phosphoethanolamine (POPE) and 1-palmitoyl-2-oleoyl-*sn*-glycero-3-phosphoglycerol (POPG), results from the nonideal mixing properties in both the gel (L_β) and the liquid-crystalline (L_α) phases.¹⁷ This behavior is attributed to hydrocarbon chain unsaturation and to differences in the interaction between the headgroups.¹⁸ It is noteworthy that POPE and POPG were selected because they mimic also the acyl chain composition found in *E. coli* inner membrane. That is, palmitic and monounsaturated acyl chains at the positions 1 and 2 of the phospholipids backbone.

In an earlier study,¹⁹ AFM provided evidence of LacY assemblies segregated in a particular domain of the phospholipid matrix after the extension of proteoliposomes of POPE and

* Corresponding author. E-mail: jordiherandezborrell@ub.edu. Tel: +34934035986.

[†] Facultat de Farmàcia, Universitat de Barcelona.

[‡] Institut de Nanociència i Nanotecnologia de la Universitat de Barcelona.

POPG at the same ratio as in the *E. coli* inner membrane. We also demonstrated, with force spectroscopy (FS), that the phospholipid segregated domains observed by AFM in SLBs of POPE:POPG can be unambiguously assigned to L_β and L_α phases.² However, these determinations were performed in bilayers of unknown lateral pressure. Hence, for a better understanding of the principles that govern LacY protein insertion in membranes, FS should be applied to POPE:POPG bilayers with defined lateral pressure and asymmetry. Here, we used the Langmuir–Blodgett (LB) method²⁰ to obtain asymmetric bilayers, where the leaflets that are proximal and distal to the mica are of different composition and different nominal lateral surface pressure. Indeed, FS mode has allowed researchers to gather additional information about the mechanics of different phospholipids monolayers and bilayers using nanometric and subnanonewton resolution (refs 1 and 2 and references therein). Therefore, the main goal of this work is to obtain quantitative information on nanomechanic properties of the monolayers of interest at a desired lateral surface pressure working in FS mode. We will compare the topography and nanomechanical properties of SLBs formed with the proximal leaflet formed by POPE or POPG and the distal leaflet formed by POPG and a mixture of both, POPE:POPG (3:1, mol/mol), with bilayers that had either the distal leaflet formed by POPE¹ or SLBs of POPE:POPG (3:1, mol/mol) mimicking the proportions of the bacterial membrane.²

Experimental Section

1-Palmitoyl-2-oleoyl-*sn*-glycero-3-phosphoethanolamine (POPE) and 1-palmitoyl-2-oleoyl-*sn*-glycero-3-phosphoglycerol (POPG), both specified as 99% pure, were purchased from Avanti Polar Lipids (Alabaster, AL). The buffer used as a subphase was 20 mM Hepes (pH 7.40), 150 mM NaCl and 20 mM CaCl₂, prepared in Ultrapure water (Milli Q reverse osmosis system, 18.3 M Ω ·cm resistivity). Chloroform and methanol, HPLC grade, were purchased from SIGMA (St. Louis, MO).

Langmuir–Blodgett films. The monolayers were prepared in a 312 DMC Langmuir–Blodgett trough manufactured by NIMA Technology Ltd. (Coventry, England). The trough was placed on a vibration-isolated table (Newport, Irvine, CA) and enclosed in an environmental chamber. The resolution of surface pressure measurement was ± 0.1 mN·m⁻¹. In all experiments, the temperature was maintained at 24.0 ± 0.2 °C by means of an external circulating water bath. Before each experiment, the trough was washed with chloroform and rinsed thoroughly with purified water.

These experiments were carried out as described in previous papers.^{21,22} The lipid was dissolved in chloroform–methanol (3:1, v/v) to a final concentration of 1 mg·mL⁻¹. The corresponding aliquot of lipid was spread onto the surface of the subphase buffer with a Hamilton microsyringe. A 15 min period was required to allow the solvent to evaporate before each experiment. The compression barrier speed was 5 cm²·min⁻¹. LB films for AFM observations were transferred at a certain surface pressure onto freshly cleaved mica, lifting the substrate at a constant rate of 1 mm·min⁻¹, thus obtaining a monolayer. Asymmetric bilayers of POPE, POPG, and a combination of the two were obtained by transferring on the downstroke a second monolayer onto the one previously obtained, as described elsewhere.²³ Specifically, asymmetric bilayers were obtained by transferring two successive monolayers of the relevant lipid onto mica, the first one in contact with the substrate, at 30 mN·m⁻¹, and the second one in contact with the buffer, at 25 mN·m⁻¹. It is important to notice that there are differences between the

nominal pressure of extraction and the real pressure of the film extracted. However, even considering large variations, both surface pressures are considered biologically relevant.²⁴ The lipid layers used as monolayer or as the second leaflet of the bilayer were left to equilibrate on the trough for 1 h before deposition. The transfer ratios were evaluated and proved near-unity, indicating that the mica was almost fully covered. The bilayers obtained were kept under buffer solution in an O-ring.

AFM Imaging. AFM experiments were performed with a Multimode microscope (Veeco, Santa Barbara, CA) controlled by Nanoscope V electronics (Veeco, Santa Barbara, CA). In the case of monolayers, images were acquired in tapping mode (TM-AFM), whereas contact mode (CM-AFM) was used for asymmetric bilayers. In both cases scanning forces were below 100 pN. V-shaped Si₃N₄ cantilevers (MSNL, Veeco, CA) with a nominal spring constant of 0.10 N·m⁻¹ were used in liquid operation, while beam-shaped silicon oxide tapping tips (37th series B cantilever, MikroMasch, Portland, OR) with a nominal spring constant of 0.3 N·m⁻¹ were used in air. Images were acquired at minimum vertical force, maximizing amplitude set point value and maintaining vibration amplitude as low as possible.

Force Spectroscopy. Force spectroscopy (FS) measurements in liquid media were performed using V-shaped Si₃N₄ tips (MSNL, Veeco, CA) with a nominal spring constant of 0.10 N·m⁻¹. However, individual spring constants were calibrated using the thermal tune method²⁵ implemented in a Multimode microscope (Digital Instruments, Santa Barbara, CA) controlled by Nanoscope V electronics (Digital Instruments, Santa Barbara, CA).

Normally, 300–400 force plots were recorded and performed, while maintaining the laser spot in the same position on the cantilever in order to keep the corresponding photodetector sensitivity (V·nm⁻¹) constant.²⁶ All spectroscopy experiments were performed at a constant cantilever linear velocity of 0.5 $\mu\text{m}\cdot\text{s}^{-1}$ in order to avoid any velocity-dependent effect. Applied forces F are given by $F = k_c \times \Delta$, where Δ is the cantilever deflection and k_c is the cantilever spring constant. The surface deformation is given as penetration (δ) evaluated as $\delta = z - \Delta$, where z represents piezo-scanner displacement. X, Y, Z piezo motion was calibrated with a DI silicon oxide grid (STR10-1800P), 180 nm deep and with 10 μm pitch.

Results and Discussion

POPE and POPG are the main components of the inner membrane of *E. coli*. The L_β -to- L_α main phase transition temperatures (T_m) for POPG, POPE and POPE:POPG (3:1, mol/mol) were established at -5.3, 23, and 23.5 °C, respectively.^{1,2,17,27} Nevertheless, in SLBs the transition encompasses a wider range of temperatures than the range observed in endotherms obtained from differential scanning calorimetry (DSC) of liposomes with the same composition.²⁸ As expected from different systems, liposomes and SLBs, the thermal transition should be different. As discussed elsewhere,²⁹ the phase transition in SLBs occurs by the individual melting of the two leaflets. This phenomenon is attributed to the existence of stabilizing interactions between the apical monolayer and the mica surface that result in turn in decoupling between both leaflets of the bilayer.¹ Accordingly, and as it has been demonstrated elsewhere,³⁰ two transition temperatures can be assigned to POPE:POPG SLBs. However, the phase shown by the bilayer as observed by AFM will be the one of the distal leaflet. Thus, while at the temperature of the AFM observations SLBs with the distal leaflet formed by POPG will show L_α phase, coexisting L_β and L_α phases will

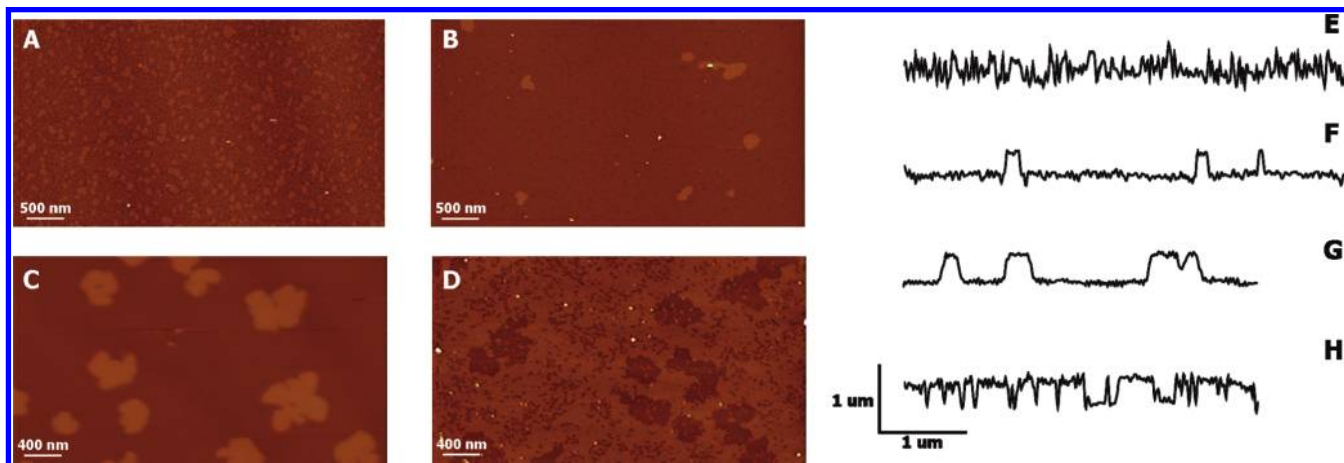


Figure 1. TM-AFM images acquired in air of monolayers of POPE at $30 \text{ mN} \cdot \text{m}^{-1}$ (A), POPG at $25 \text{ mN} \cdot \text{m}^{-1}$ (B), POPG at $30 \text{ mN} \cdot \text{m}^{-1}$ (C), and POPE:POPG (3:1, mol/mol) at $25 \text{ mN} \cdot \text{m}^{-1}$ (D). E–H are representative line profile analysis of the images A–D. Buffer: 20 mM Hepes, 150 mM NaCl, 20 mM of CaCl_2 (pH 7.40). The monolayers were transferred onto mica on the upstroke. The z color scale is 15 nm, and the scale bar is $5 \mu\text{m}$ for A and B and $4 \mu\text{m}$ for C and D.

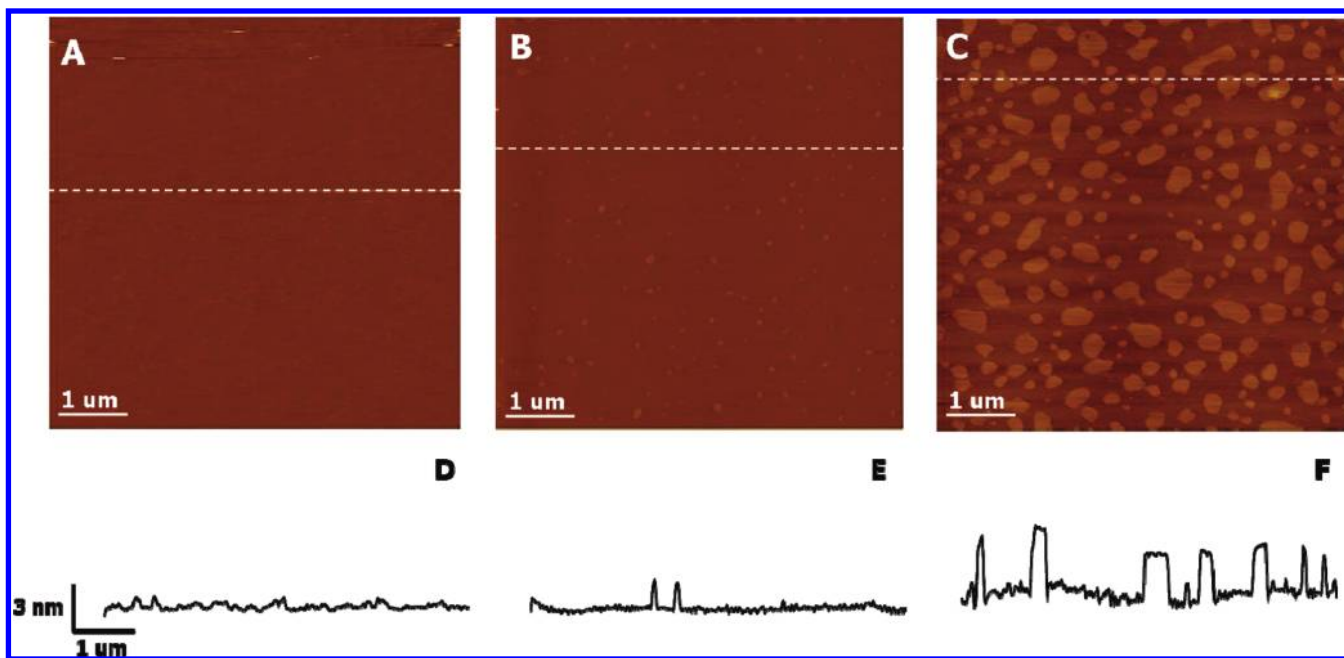


Figure 2. CM-AFM images acquired in liquid of asymmetric bilayers of POPG/POPG ($30/25 \text{ mN} \cdot \text{m}^{-1}$) (A), POPE/POPG ($30/25 \text{ mN} \cdot \text{m}^{-1}$) (B); and POPE/POPE:POPG (3:1, mol/mol) ($30/25 \text{ mN} \cdot \text{m}^{-1}$) (C). Buffer: 20 mM Hepes, 150 mM NaCl, 20 mM CaCl_2 (pH 7.40). The proximal monolayers were transferred onto cleaved mica on the upstroke, whereas the transfer of the distal monolayers was carried out on the downstroke. The z color scale is 30 nm, and the scale bar is $6 \mu\text{m}$.

be distinguished in SLBs with the distal leaflet formed by POPE:POPG (3:1, mol/mol).

In analogy with the main transition undergone by phospholipid bilayers, pressure/area isotherms of phospholipid monolayers are characterized by a main transition between the liquid-expanded (LE) and the liquid-condensed (LC) phases. Thus, according to the compression isotherms published elsewhere,^{1,21,31,32} both phospholipids are in LE phase at the surface pressures of the extraction. However, AFM images provide a better insight into the nanostructure of LB monolayers, and coexisting phases, LE and LC, can be distinguished at a defined surface pressure.

Figure 1 shows the AFM topographic images acquired in air and the cross-section analysis performed at the lines drawn in the images of the LB monolayers used for the formation of asymmetric bilayers. Figure 1A shows the LB monolayer of POPE extracted at $30 \text{ mN} \cdot \text{m}^{-1}$. As previously reported,^{21,33}

small LC microdomains surrounded by the LE phase can be seen. Panels B and C of Figure 1 correspond to AFM topographic images of POPG monolayers extracted at 25 and $30 \text{ mN} \cdot \text{m}^{-1}$, respectively. As can be seen, the LC domains for POPG are larger than those observed for POPE and increase in number and size with surface pressure. Binding of Ca^{2+} to negatively charged phospholipids such as POPG induces an isothermal formation of large clusters formed by Ca^{2+} –POPG within the LE domain.³⁴ This phenomenon does not occur with zwitterionic phospholipids like POPE, which explains the small size of the LC domains in Figure 1A. In turn, the POPE:POPG (3:1, mol/mol) monolayer extracted at $25 \text{ mN} \cdot \text{m}^{-1}$ shows coexisting LC and LE domains. Since both phospholipids show nonideal mixing properties, the composition of each domain is unknown. However, the propensity of POPG to form clusters in presence of Ca^{2+} suggests that the LC domains are enriched in this phospholipid.

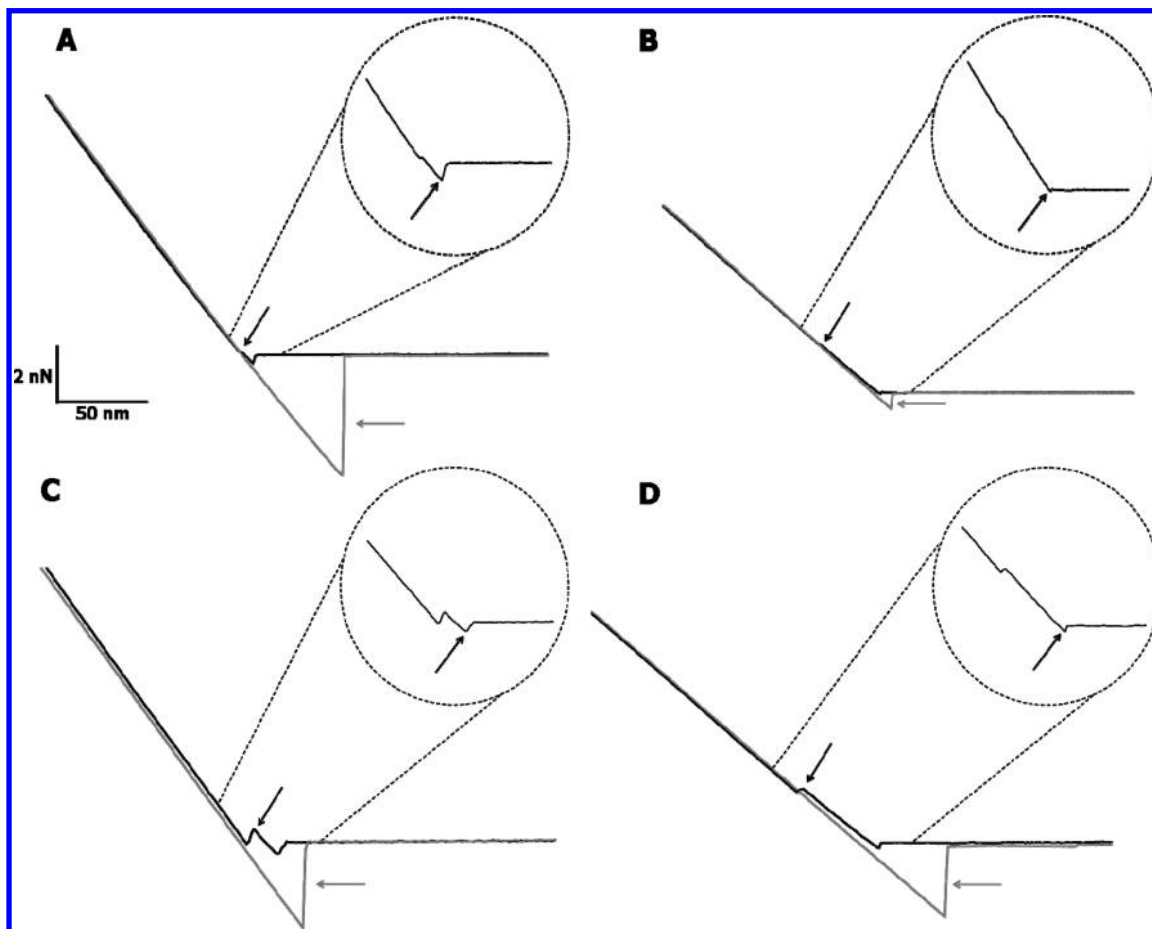


Figure 3. Representative vertical force versus piezo displacement curves (F_v – D) performed along the asymmetric bilayers shown in Figure 2: POPG/POPG (30/25 mN m^{-1}) (A), POPE:POPG (30/25 mN m^{-1}) (B); and L_α phase (C) and L_β phase (D) of POPE/POPE:POPG (30/25 mN m^{-1}). The approaching part of the curve displaying the breakthrough force is depicted in black, whereas the retracting part of the curve showing the adhesion force is in gray. The highlighted region of each force curve is magnified (dashed circle) showing the jump-to-contact present in F_v – D plots. Black and gray arrows point out the features observed in each force curve in the approach and retract region, respectively.

AFM images acquired in a liquid of different asymmetric bilayers obtained with the blistered monolayers are shown in Figure 2. The topographic image of the POPG/POPG bilayer (POPG in the L_α phase) with the proximal and distal leaflets extracted at 30 and 25 mN m^{-1} , respectively, is shown in Figure 2A. Although the existence of domains in both leaflets has been observed in air (Figure 1, B and C), the distal bilayer, the one observed, is featureless and smooth, as revealed by the cross-section analysis (Figure 2D). The POPE/POPG bilayer (POPG in the L_α phase) (Figure 2B), formed by the first leaflet extracted at 25 mN m^{-1} and the second leaflet extracted at 30 mN m^{-1} , shows small domains that can be better appreciated in the cross-section analysis (Figure 2E). Figure 2C is an AFM topographic image of a POPE/POPE:POPG bilayer. This asymmetrical bilayer was formed by extraction of the proximal leaflet, POPE, at 25 mN m^{-1} and the distal leaflet, POPE:POPG (3:1, mol/mol) (coexisting L_β and L_α phase), at 30 mN m^{-1} . Therefore, two domains can be clearly distinguished, with a step-height difference (see cross-section analysis in Figure 2F) of 2.47 ± 0.147 nm. It is quite possible that this value might be overestimated as a result of the repulsion between the tip and the negative charge due to the relative enrichment in POPG of the L_α phase. An indirect evidence of such enrichment can be obtained from the analysis of the phase diagram of the POPE:POPG system in liposomes.¹⁴

The physicochemical properties of the proximal monolayer (Figure 1A) may affect the nanostructure of the distal leaflets.

Thus, in Figure 2B,C, domains are probably smaller than might be expected from the size of the domains observed in the monolayers used to form the apical leaflet (Figure 1). However, caution should be exercised when comparing the features of monolayers (Figure 1) and bilayers (Figure 2). Actually, while Figure 1 shows the acyl chains in air, Figure 2 shows the headgroups in liquid. It is possible that during or after the blistering process, molecules from the first leaflet extracted might migrate to the second leaflet and vice versa, producing a molecular rearrangement of the system, as observed elsewhere.³⁵

TABLE 1: Mean Value of the F_y and F_{adh} of Different Asymmetric Bilayers and SLBs of POPE, POPG, and a Mixture of Both, Mimicking the Composition of the Inner Membrane of *E. coli* as well as of DMPC, a Less Physiological Phospholipid Which Is Shown Here for Comparison

proximal leaflet 30 mN m^{-1}	distal leaflet 25 mN m^{-1}		F_y (nN)	F_{adh} (nN)
POPE	POPG		1.64 ± 0.06	0.45 ± 0.03
POPG	POPG		0.58 ± 0.02	4.95 ± 0.08
POPE	POPE/POPG 3/1 (mol/mol)	L_α	0.62 ± 0.04	3.31 ± 0.06
		L_β	2.18 ± 0.05	2.23 ± 0.06
POPE ¹	POPE ¹		1.76 ± 0.11	3.00 ± 0.26
SLB POPE/POPG ¹ 3/1 (mol/mol)	SLB POPE/POPG ¹ 3/1 (mol/mol)	L_α	0.24 ± 0.07	1.58 ± 0.13
		L_β	0.91 ± 0.19	0.24 ± 0.06
SLB DMPC ²²	SLB DMPC ²²		14.93 ± 0.09	data not available

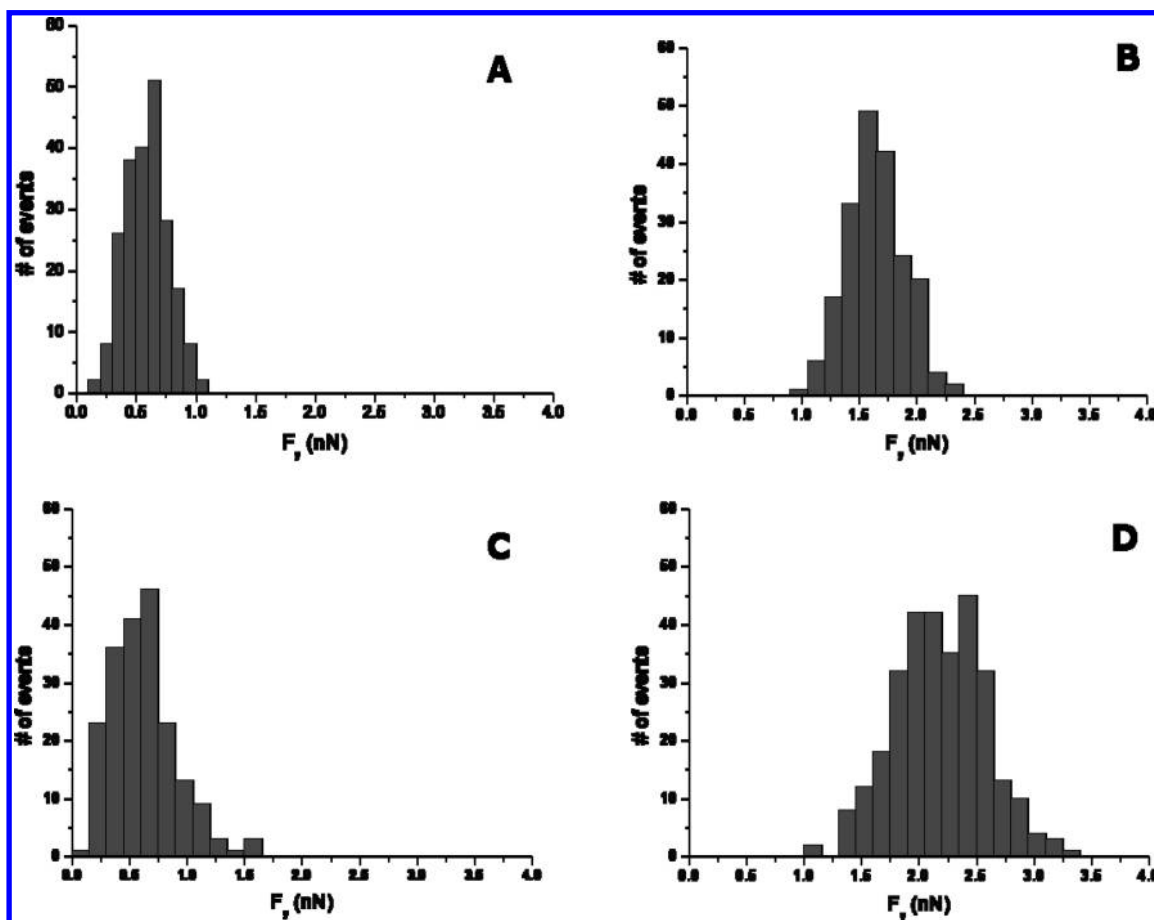


Figure 4. Histograms of the experimental F_y values obtained after processing Fv – D curves shown in Figure 2: POPG/POPG (30/25 mN m^{-1}) (A), POPE:POPG (30/25 mN m^{-1}) (B); and L_α phase (C) and L_β phase (D) of POPE/POPE:POPG (30/25 mN m^{-1}).

The distal leaflet in Figure 2C displays similar lateral phase separation to SLBs formed by spreading liposomes onto mica.² The step-height difference between the two phases is, however, higher for the SLBs formed by the LB technique. Since the same lateral separation phenomenon occurs regardless of the method used to obtain the planar bilayer, we conclude that Figure 2C shows L_β and L_α phases.

FS has emerged as a powerful tool for providing quantitative information on the nanostructure and nanomechanics of phospholipid monolayers and bilayers.^{36–38} This information enables the characterization of biomembranes with different physicochemical characteristics, i.e. discrimination between coexisting L_β and L_α phases of the same SLB.^{2,35,37} Figure 3 shows the examples of the vertical force versus piezo displacement curves (Fv – D) performed in the SLBs described in Figure 2. From these curves, two main items of information can be extracted: (i) the breakthrough or threshold force (F_y), i.e., the force that the bilayer can withstand before being indentate; and (ii) the adhesion force (F_{adh}) between the tip and the bilayer. In the force curves, F_y appears as a jump in the attractive regime, the approaching part of the curve, at higher forces that the jump-to-contact; whereas the magnitude of F_{adh} is extracted in the repulsive regime, from the retracting part of the curve. The jump-to-contact, when the attractive forces overcome the spring constant of the cantilever and the repulsive forces, was observed in our experiment in all cases (Figure 3). However, the jump-to-contact is not always observed in liquid.³⁹ These observations in our experiments can be attributed to the presence of a high concentration of Ca^{2+} .

The values of F_y were lower for the POPG/POPG bilayer (Figure 3A) than for the POPE/POPG bilayer (Figure 3B). As

can be seen in Table 1, these values are even lower than those obtained for the asymmetric bilayer of POPE/POPE,¹ suggesting indeed the effect that the proximal layer has on the nanomechanical properties of the system. The distributions of the values for the POPG/POPG and POPE/POPG bilayers are shown in Figure 4, A and B. The mean F_y values were 0.58 ± 0.02 and 1.64 ± 0.06 nN, respectively (Table 1). The F_y value for the asymmetric POPE:POPG bilayers is similar to the value obtained for the POPE:POPE bilayers¹ and higher than that obtained for the POPG:POPG bilayer (Table 1). These findings indicate that the proximal leaflet may influence the distal one.

Figure 3, C and D, shows representative Fv – D curves for the L_α and L_β phases observed in Figure 2C. As expected from the inherent physicochemical properties of each phase, the F_y values were higher for the L_β than for the L_α phase (see Figure 4, C and D). More generally, this reflects the differences in the nanomechanical behavior of each phase. Interestingly, the mean F_y values found, 0.62 ± 0.04 and 2.18 ± 0.05 nN for the L_α and L_β phases, respectively, are slightly higher than those reported for both phases in SLBs of POPE:POPG² formed by vesicle fusion onto mica (Table 1). This can be interpreted as a result of the higher lateral pressure of the SLBs formed by LB deposition.

As shown in Figure 3, the adhesive forces were substantially different in their bilayer composition. The magnitudes of F_{adh} values obtained for each bilayer and their frequencies are seen in the histograms shown in Figure 5. The mean values of F_{adh} were higher for the POPG/POPG bilayer (4.95 ± 0.08 nN) than for the POPE/POPG bilayer (0.45 ± 0.03 nN) (see Table 1). Since both asymmetric bilayers have the same composition and surface pressure for the distal leaflet (POPG), these results

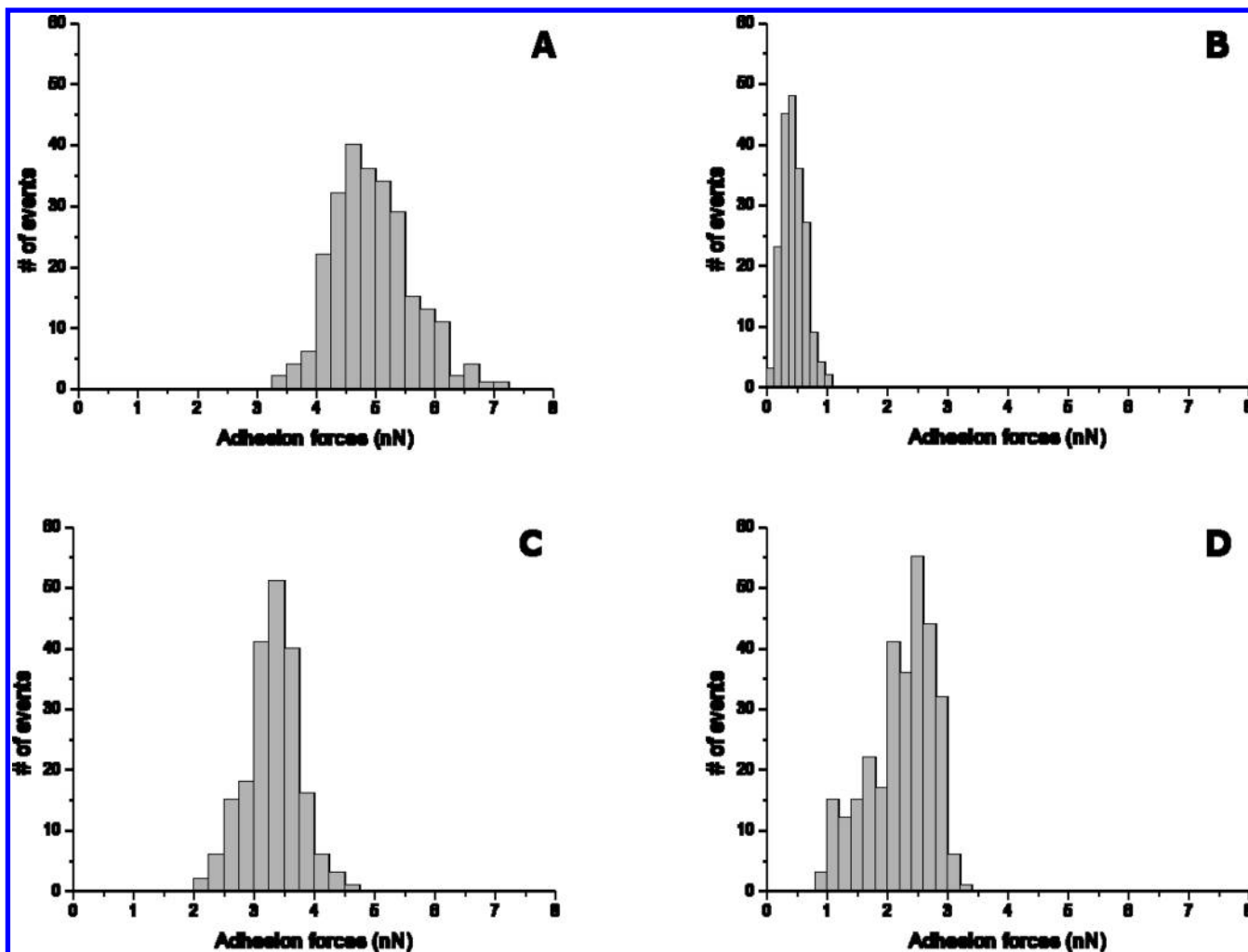


Figure 5. Histograms of the experimental F_{adh} values obtained after processing F_v - D curves shown in Figure 2: POPG/POPG ($30/25 \text{ mN m}^{-1}$) (A), POPE:POPG ($30/25 \text{ mN m}^{-1}$) (B); and L_α phase (C) and L_β phase (D) of POPE/POPE:POPG ($30/25 \text{ mN m}^{-1}$).

suggest that the adhesive forces depend on the composition of the proximal layer, POPG and POPE, respectively, extracted at 30 mN m^{-1} (see Figure 2A,B). The magnitudes of F_{adh} obtained for the L_α and L_β phases shown in Figure 2 and their frequencies are shown in histograms C and D in Figure 5. The mean values for each phase were established at 3.31 ± 0.06 and $2.23 \pm 0.06 \text{ nN}$ (Table 1). These results are consistent with the observation that higher F_{adh} values are expected from fluid phases. That is, fluid phases display higher adhesive pull-off forces than gel phases as has been extensively reported.^{36,37} In this sense, if we assume that the monolayer directly interacting with the mica is the one that mainly governs the nanomechanics of the system, it is reasonable to expect lower adhesion forces when PE is the underlying monolayer. Under our experimental conditions, POPE is most likely below the transition temperature and so displaying the L_β phase, whereas POPG is in L_α phase. This would explain why F_{adh} obtained in the POPE/POPE:POPG bilayer are lower than for POPG/POPG bilayer. In the case of values reported from POPE/POPE bilayer, studies¹ performed were carried out above the L_β to L_α transition so this also would explain why the obtained F_{adh} values are also higher.

As discussed elsewhere,⁴⁰ many membrane proteins show preference for phospholipids in the fluid phase because they provide better packing properties for the protein surface. Thus, there was earlier evidence that LacY tends to locate in the L_α phase.⁴¹ Notice that, as shown in Table 1, phospholipids in the fluid phase have different nanomechanical properties than in

the gel phase. Since LacY is fully functional when reconstituted into POPE:POPG (3:1, mol/mol), it is reasonable to assume that the protein is inserted in the L_α phase. Confirming such assumption, we have recently shown by using AFM⁴² that LacY, indeed, inserts preferentially into fluid domains of POPE:POPG SLBs. Consequently, we can infer that the protein is inserted in the phase with the lower F_y , and the higher F_{adh} . Actually, this is consistent with the idea that the insertion of proteins in the membrane depends not only on the fluidity of phospholipids but also on the nanomechanical properties of the membrane, which depends in turn on lateral compressibility. Thus, in an earlier study on LacY insertion in SLBs of POPE:POPG (3:1, mol/mol)¹⁹ we observed protein-assembled segregated domains. There, we suggested that these domains were formed as a consequence of the specific affinity of LacY for a particular phospholipid phase. Now, in view of the results shown in the present paper, we can conclude that this affinity seems related with the nanomechanical properties of this phospholipid phase. The information gathered here from nanomechanical properties of POPE:POPG bilayers should be used for further studies aimed at investigating this preferential insertion of LacY in fluid domains and, in particular, at clarifying how this relates to the composition of the annular region.¹¹ Experiments along these lines have been recently undertaken in our laboratory.

Acknowledgment. L.P. is the recipient of an APIF fellowship from the University of Barcelona. C.S.-G. is the recipient of a

fellowship of the Ministerio de Ciencia e Innovación. Thanks to Dr. Gerard Oncins of the Serveis Científic-Tècnics de la UB for helping in the discussion. This study was supported by Grant CTQ-2008-03922/BQU from Spain's Ministerio de Ciencia e Innovación (Spain).

References and Notes

- (1) Picas, L.; Montero, M. T.; Morros, A.; Oncins, G.; Hernandez-Borrell, J. Phase Changes in Supported Planar Bilayers of 1-Palmitoyl-2-Oleoyl-*sn*-Glycerol-3 Phosphoethanolamine. *J. Phys. Chem. B* **2008**, *112*, 10181–10187.
- (2) Picas, L.; Montero, M. T.; Morros, A.; Cabanas, M. E.; Seantier, B.; Milhiet, P. E.; Hernandez-Borrell, J. Calcium-Induced Formation of Subdomains in Phosphatidylethanolamine-Phosphatidylglycerol Bilayers: A Combined DSC, ³¹P NMR, and AFM Study. *J. Phys. Chem. B* **2009**, *113*, 4648–4655.
- (3) Mitchell, P. Molecule, Group and Electron Translocation through Natural Membranes. *Biochem. Soc. Symp.* **1963**, *22*, 142–168.
- (4) Mitchell, P. In *Chemiosmotic coupling and energy transduction*; Glynn Research Ltd.: Bodmin, UK, 1968.
- (5) Guan, L.; Smirnova, I. N.; Verner, G.; Nagamori, S.; Kaback, H. R. Manipulating Phospholipids for Crystallization of a Membrane Transport Protein. *Proc. Natl. Acad. Sci. U.S.A.* **2006**, *103*, 1723–1726.
- (6) Warren, G. B.; Toon, P. A.; Birdsall, N. J.; Lee, A. G.; Metcalfe, J. C. Reversible Lipid Titrations of the Activity of Pure Adenosine Triphosphatase-Lipid Complexes. *Biochemistry* **1974**, *13*, 5501–5507.
- (7) Dumas, F.; Toccanne, J. F.; Leblanc, G.; Lebrun, M. C. Consequences of Hydrophobic Mismatch between Lipids and Melibiose Permease on Melibiose Transport. *Biochemistry* **2000**, *39*, 4846–4854.
- (8) Dowhan, W.; Bogdanov, M. Lipid-Dependent Membrane Protein Topogenesis. *Annu. Rev. Biochem.* **2009**, *78*, 515–540.
- (9) Gbaguidi, B.; Hakizimana, P.; Vandenbussche, G.; Ruysschaert, J. M. Conformational Changes in a Bacterial Multidrug Transporter are Phosphatidylethanolamine-Dependent. *Cell Mol. Life Sci.* **2007**, *64*, 1571–1582.
- (10) Valiyaveetil, F. I.; Zhou, Y.; MacKinnon, R. Lipids in the Structure, Folding, and Function of the KcsA K⁺ Channel. *Biochemistry* **2002**, *41*, 10771–10777.
- (11) Picas, L.; Montero, M. T.; Morros, A.; Vazquez-Ibar, J. L.; Hernandez-Borrell, J. Evidence of Phosphatidylethanolamine and Phosphatidylglycerol Presence at the Annular Region of Lactose Permease of *Escherichia Coli*. *Biochim. Biophys. Acta* **2009**, (DOI:10.1016/j.bbamem.2009.06.024).
- (12) Dowhan, W. Molecular basis for membrane phospholipid diversity: Why are there so many lipids? *Annu. Rev. Biochem.* **1997**, *66*, 199–232.
- (13) Morein, S.; Andersson, A. S.; Rikfors, L.; Lindblom, G. Wild-type *Escherichia coli* cells regulate the membrane lipid composition in a “window” between gel and non-lamellar structure. *J. Biol. Chem.* **1996**, *271*, 6801–6809.
- (14) Haines, T. H.; Dencher, N. A. Cardiolipin: A Proton Trap for Oxidative Phosphorylation. *FEBS Lett.* **2002**, *528*, 35–39.
- (15) Zerrouk, Z.; Alexandre, A.; Lafontaine, C.; Norris, V.; Valleton, J. M. Inner membrane lipids of *Escherichia coli* form domains. *Colloids Surf. B: Biointerfaces* **2008**, *63*, 306–310.
- (16) Mileykovskaya, E.; Fishov, I.; Fu, X.; Corbin, B. D.; Margolin, W.; Dowhan, W. Effects of Phospholipid Composition on MinD-Membrane Interactions in Vitro and in Vivo. *J. Biol. Chem.* **2003**, *278*, 22193–22198.
- (17) Pozo Navas, B.; Lohner, K.; Deutsch, G.; Sevcik, E.; Riske, K. A.; Dimova, R.; Garidel, P.; Pabst, G. Composition Dependence of Vesicle Morphology and Mixing Properties in a Bacterial Model Membrane System. *Biochim. Biophys. Acta* **2005**, *1716*, 40–48.
- (18) Murzyn, K.; Rog, T.; Pasenkiewicz-Gierula, M. Phosphatidylethanolamine-Phosphatidylglycerol Bilayer as a Model of the Inner Bacterial Membrane. *Biophys. J.* **2005**, *88*, 1091–1103.
- (19) Merino, S.; Domenech, O.; Vinas, M.; Montero, M. T.; Hernandez-Borrell, J. Effects of Lactose Permease on the Phospholipid Environment in which it is Reconstituted: A Fluorescence and Atomic Force Microscopy Study. *Langmuir* **2005**, *21*, 4642–4647.
- (20) Mingot-Leclercq, M. P.; Deleu, M.; Brasseur, R.; Dufrene, Y. F. Atomic Force Microscopy of Supported Lipid Bilayers. *Nat. Protoc.* **2008**, *3*, 1654–1659.
- (21) Domenech, O.; Ignes-Mullol, J.; Montero, M. T.; Hernandez-Borrell, J. Unveiling a Complex Phase Transition in Monolayers of a Phospholipid from the Annular Region of Transmembrane Proteins. *J. Phys. Chem. B* **2007**, *111*, 10946–10951.
- (22) Garcia-Manyes, S.; Domenech, O.; Sanz, F.; Montero, M. T.; Hernandez-Borrell, J. Atomic Force Microscopy and Force Spectroscopy Study of Langmuir-Blodgett Films Formed by Heteroacid Phospholipids of Biological Interest. *Biochim. Biophys. Acta* **2007**, *1768*, 1190–1198.
- (23) Rinia, H. A.; Demel, R. A.; van der Eerden, J. P. J. M.; de Kruijff, B. Blistering of Langmuir-Blodgett Bilayers Containing Anionic Phospholipids as Observed by Atomic Force Microscopy. *Biophys. J.* **1999**, *77*, 1683–1693.
- (24) Cevc, G.; Marsh, D. In *Phospholipid Bilayers. Physical Principles and Models*; Wiley-Interscience: New York, 1987.
- (25) Florin, E. L.; Rief, M.; Lehmann, H.; Ludwig, M.; Dornmair, C.; Moy, V. T.; Gaub, H. E. Sensing specific molecular interactions with the atomic force microscope. *Biosens. Bioelectron.* **1995**, *10*, 895–901.
- (26) Proksch, R.; Schaffer, T. E.; Cleveland, J. P.; Callahan, R. C.; Viani, M. B. Finite Optical Spot Size and Position Corrections in Thermal Spring Constant Calibration. *Nanotechnology* **2004**, *15*, 1344–1350.
- (27) Fleming, B. D.; Keough, K. M. Thermotropic Mesomorphism in Aqueous Dispersions of 1-Palmitoyl-2-Oleoyl- and 1,2-Dilauroyl-Phosphatidylglycerols in the Presence of Excess Na⁺ Or Ca²⁺. *Can. J. Biochem. Cell Biol.* **1983**, *61*, 882–891.
- (28) Keller, D.; Larsen, N. B.; Moller, I. M.; Mouritsen, O. G. Decoupled Phase Transitions and Grain-Boundary Melting in Supported Phospholipid Bilayers. *Phys. Rev. Lett.* **2005**, *94*, 025701.
- (29) Oncins, G.; Picas, L.; Hernandez-Borrell, J.; Garcia-Manyes, S.; Sanz, F. Thermal Response of Langmuir-Blodgett Films of Dipalmitoylphosphatidylcholine Studied by Atomic Force Microscopy and Force Spectroscopy. *Biophys. J.* **2007**, *93*, 2713–2725.
- (30) Seeger, H. M.; Marino, G.; Alessandrini, A.; Facci, P. Effect of physical parameters on the main phase transition of supported lipid bilayers. *Biophys. J.* **2009**, *97*, 1067–1076.
- (31) Takamoto, D. Y.; Lipp, M. M.; von Nahmen, A.; Lee, K. Y.; Waring, A. J.; Zasadzinski, J. A. Interaction of Lung Surfactant Proteins with Anionic Phospholipids. *Biophys. J.* **2001**, *81*, 153–169.
- (32) Diemel, R. V.; Snel, M. M.; Waring, A. J.; Walther, F. J.; van Golde, L. M.; Putz, G.; Haagsman, H. P.; Batenburg, J. J. Multilayer Formation upon Compression of Surfactant Monolayers Depends on Protein Concentration as Well as Lipid Composition. an Atomic Force Microscopy Study. *J. Biol. Chem.* **2002**, *277*, 21179–21188.
- (33) Saulnier, P.; Foussard, F.; Boury, F.; Proust, J. E. Structural Properties of Asymmetric Mixed-Chain Phosphatidylethanolamine Films. *J. Colloid Interface Sci.* **1999**, *218*, 40–46.
- (34) Houslay, M. D.; Stanley, K. K. In *Dynamics of Biological Membranes, influence on synthesis, structure and function*; Wiley Interscience: New York, 1982.
- (35) Goksu, E. I.; Vanegas, J. M.; Blanchette, C. D.; Lin, W. C.; Longo, M. L. AFM for Structure and Dynamics of Biomembranes. *Biochim. Biophys. Acta* **2009**, *1788*, 254–266.
- (36) Dufrene, Y. F.; Barger, W. R.; Green, J. B. D.; Lee, G. U. Nanometer-Scale Surface Properties of Mixed Phospholipid Monolayers and Bilayers. *Langmuir* **1997**, *13*, 4779–4784.
- (37) Dufrene, Y. F.; Boland, T.; Schneider, J. W.; Barger, W. R.; Lee, G. U. Characterization of the Physical Properties of Model Biomembranes at the Nanometer Scale with the Atomic Force Microscope. *Faraday Discuss.* **1998**, *79*–94.
- (38) Garcia-Manyes, S.; Oncins, G.; Sanz, F. Effect of Ion-Binding and Chemical Phospholipid Structure on the Nanomechanics of Lipid Bilayers Studied by Force Spectroscopy. *Biophys. J.* **2005**, *89*, 1812–1826.
- (39) Muller, D. J.; Engel, A. The Height of Biomolecules Measured with the Atomic Force Microscope Depends on Electrostatic Interactions. *Biophys. J.* **1997**, *73*, 1633–1644.
- (40) Lee, A. G. Lipid-Protein Interactions in Biological Membranes: A Structural Perspective. *Biochim. Biophys. Acta* **2003**, *1612*, 1–40.
- (41) Thilo, L.; Trauble, H.; Overath, P. Mechanistic Interpretation of the Influence of Lipid Phase Transitions on Transport Functions. *Biochemistry* **1977**, *16*, 1283–1290.
- (42) Picas, L.; Carretero-Genevri, A.; Montero, M. T.; Vázquez-Ibar, J. L.; Seantier, B.; Milhiet, P. E.; Hernandez-Borrell, J. Preferential insertion of lactose permease in phospholipid domains: AFM observations. *Biochim. Biophys. Acta* (doi: 10.1016/j.bbamem.2010.01.008)